Supplementary information for

Computational Investigation of High Stability and Solar-to-Hydrogen Efficiency in Two-Dimensional SiP, GeP, and SnP for Enhanced Photocatalytic Water Splitting

Calculation methods

(1) Young's modulus and Poisson's ratio

For two-dimensional materials, the in-plane Young's modulus ($Y(\theta)$) and Poisson's ratio ($\upsilon(\theta)$) can be calculated using its elastic constant (C_{ij}) and the angle (θ) with respect to the *a*-axis, as follows[1, 2]:

$$Y(\theta) = \frac{C_{11}C_{22} - C_{12}^2}{C_{11}\sin^4\theta + (\frac{C_{11}C_{22} - C_{12}^2}{C_{66}} - 2C_{12})\sin^2\theta\cos^2\theta + C_{22}\cos^4\theta}$$

(S1)

$$\upsilon(\theta) = \frac{C_{12}\sin^4\theta - (C_{11} + C_{22} - \frac{C_{11}C_{22} - C_{12}^2}{C_{66}})\sin^2\theta\cos^2\theta + C_{12}\cos^4\theta}{C_{11}\sin^4\theta + (\frac{C_{11}C_{22} - C_{12}^2}{C_{66}} - 2C_{12})\sin^2\theta\cos^2\theta + C_{22}\cos^4\theta}$$

(S2)

(2) Carrier mobility

For two-dimensional materials, the carrier mobility (μ) can be estimated using the deformation potential theory (DPT)[3-5], and the calculation

formula can be expressed as $\mu = \frac{e\hbar^2 C^{2D}}{k_B T m^* m_d E_l^2}$, where C^{2D} is the two-dimensional elastic modulus, m^* is the effective mass along the transport direction, m_d is the density-of-states effective mass defined as $m_d = \sqrt{m_a^* m_b^*}$, and E_l is the deformation potential constant defined by $E_l = \partial E_{edge}/\partial E$; E_{edge} is the conduction band minima (for electrons) and valence band maxima (for holes) and E is the uniaxial strain along the transport direction. Here we set the total uniaxial strain is -4% ~ 4% and with the step size of 2%.

(3) Gibbs free energy

We calculated the Gibbs free energy (ΔG) for the adsorption of intermediates (*H, *OH, *O, and *OOH) on the surface of the monolayer during the photocatalytic water splitting process, governed by the following relationships:[6]

$$\Delta G = \Delta E + \Delta E_{ZPE} - T\Delta S + \Delta G_{pH} - eU \quad \text{(S3)}$$

Where ΔE represents the differential adsorption energy for each intermediate reaction, and ΔE_{ZPE} is the difference in zero-point energy (*ZPE*). *T* denotes the temperature of 298.15 K, while ΔS represents the entropy change obtained from vibrational frequency calculations. ΔG_{pH} accounts for the change in free energy influenced by the pH value. *U* is the electrode potential relative to the standard water reduction potential.

Also, at ambient temperature, the expression for $T\Delta S$ is approximately

−0.24 eV. Therefore, the Gibbs free energy *G of *H can be simplified as follows:[7]

$$\Delta G_{*H} = \Delta E + 0.24 \qquad \text{(S4)}$$

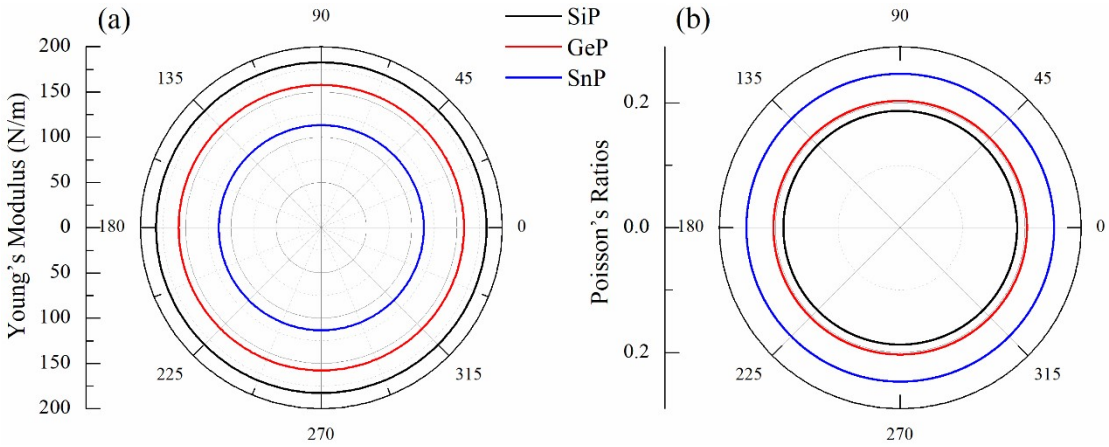

Fig. S1 (a) Young's modulus and (b) Poisson's ratio for three monolayers. The black, red, and green curves represent SiP, GeP, and SnP, respectively. The angles are measured relative to the z-axis direction.

Table S1 The results of Bader charge analysis of three monolayers.

Materials	Si/Ge/Sn (|*e*|)	P (|*e*|)
SiP	+1.13	1.13
GeP	+0.63	0.63
SnP	+0.45	0.45

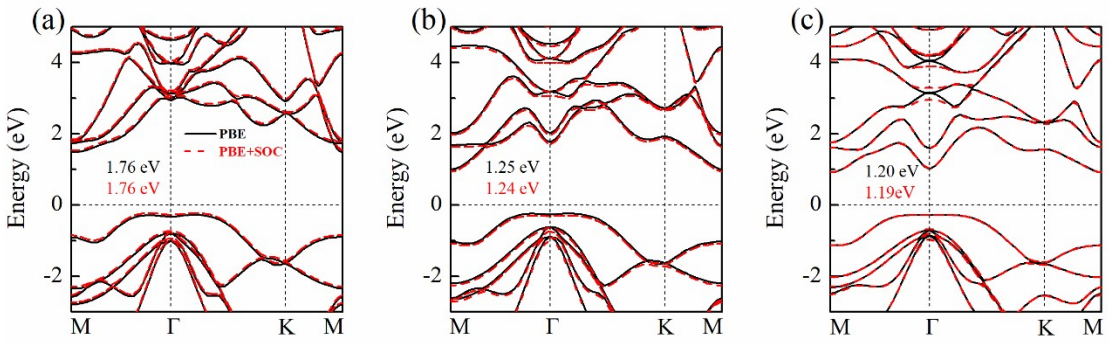

Fig. S2 Band structures of (a) SiP, (b) GeP, and (c) SnP under GGA - PBE functional with (red line) and without SOC (black line).

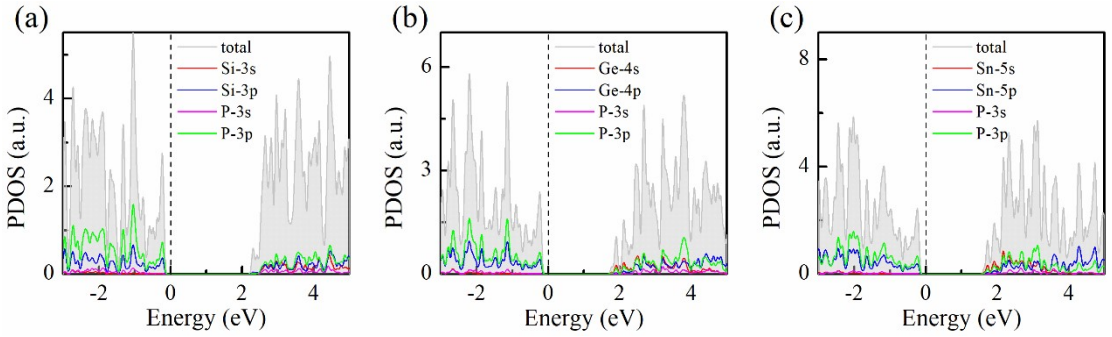

Fig. S3 Partial density of states of (a) SiP, (b) GeP, and (c) SnP under HSE06 functional, with the Fermi level set at 0 eV.

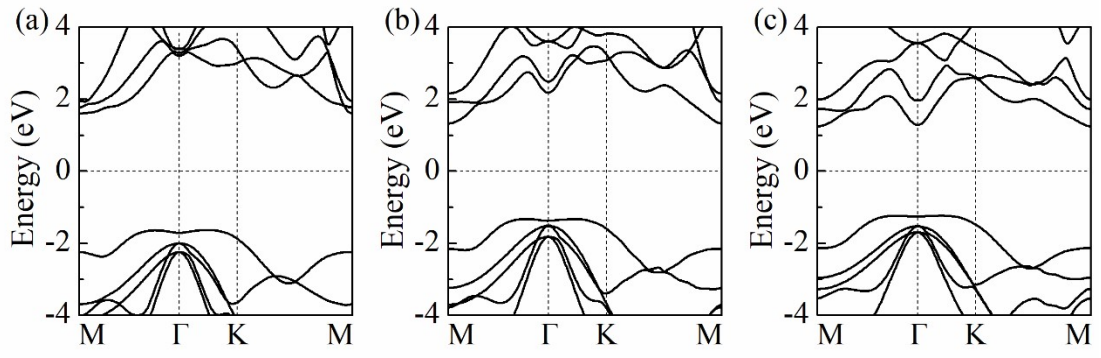

Fig. S4 Quasiparticle band structures of (a) SiP, (b) GeP, and (c) SnP calculated by GW0+Wannier approximation.

Table S2 The total energy E_t, the position of VBM (E_V) and CBM (E_C) with respect to vacuum level (VL) at uniaxial strains of -4% ~ 4%, where the step size is 2%.

Monolayers	Strain	E_t (eV)	E_V (eV)	E_C (eV)	VL (eV)
SiP	-4%	-22.195	-5.940	-4.262	4.106
	-2%	-22.210	-5.924	-4.203	4.080
	0%	-22.214	-5.905	-4.144	4.054
	2%	-22.210	-5.874	-4.271	4.028
	4%	-22.196	-5.845	-4.391	4.002
GeP	-4%	-19.743	-5.804	-4.586	3.880
	-2%	-19.757	-5.781	-4.550	3.854
	0%	-19.762	-5.760	-4.515	3.830
	2%	-19.759	-5.728	-4.555	3.804
	4%	-19.747	-5.697	-4.604	3.778
SnP	-4%	-18.182	-5.694	-4.500	4.322
	-2%	-18.194	-5.670	-4.473	4.293
	0%	-18.198	-5.646	-4.447	4.265
	2%	-18.195	-5.616	-4.476	4.237
	4%	-18.184	-5.587	-4.516	4.209

Table S3 The calculation details of the Gibbs free energy change of the intermediate product in monolayer GeP during the HER. Here, E_{DFT} represents the total energy of the intermediate product adsorbed at the most probable position on the superlattice surface, G_{tot} represents the total Gibbs free energy, and the *T* is set to 298.15 K.

Materials	E_{DFT}	G_{tot}	$\Delta G(U = 0.0\ V)$	$\Delta G(U = 1.23\ V)$
SiP	-196.441	-194.582	1.784	0.555
GeP	-174.135	-172.014	1.522	0.292
SnP	-161.661	-159.228	1.210	-0.020

Table S4 The calculation details of the Gibbs free energy change of the intermediate product in monolayer SiP during the OER. Here, E_{DFT} represents the total energy of the intermediate product adsorbed at the most probable position on the superlattice surface, G_{tot} represents the total Gibbs free energy, and the *T* is set to 298.15 K.

Materials	E_{DFT}	ΔE_{zpe}	$T\Delta S$	Molecular	G_{tot}	$\Delta G(U = 0.0\ V)$	$\Delta G(U = 1.23\ V)$
G*	-194.582	0.000	0.000	H_2O	-223.050	0.000	0.000
G*OH	-204.000	0.325	0.094	$H_2O + (H^+ + e^-)$	-221.406	1.644	0.414
G*O	-200.762	0.076	0.065	$H_2O + 2(H^+ + e^-)$	-221.792	1.259	-1.201
G*OOH	-207.841	0.398	0.153	$3(H^+ + e^-)$	-217.807	5.244	1.554
G*	-194.582	0.000	0.000	$O_2 + 4(H^+ + e^-)$	-218.130	4.920	0.000

Table S5 The calculation details of the Gibbs free energy change of the intermediate product in monolayer GeP during the OER. Here, E_{DFT} represents the total energy of the intermediate product adsorbed at the most probable position on the superlattice surface, G_{tot} represents the total Gibbs free energy, and the *T* is set to 298.15 K.

Materials	E_{DFT}	ΔE_{zpe}	$T\Delta S$	Molecular	G_{tot}	$\Delta G(U = 0.0\ V)$	$\Delta G(U = 1.23\ V)$
G*	-172.014	0.000	0.000	H_2O	-200.482	0.000	0.000
G*OH	-181.767	0.326	0.093	$H_2O + (H^+ + e^-)$	-199.171	1.311	0.081

G*O	-178.642	0.076	0.067	$H_2O + 2(H^+ + e^-)$	-199.674	0.808	-1.652
G*OOH	-185.964	0.362	0.189	$3(H^+ + e^-)$	-196.001	4.481	0.791
G*	-172.014	0.000	0.000	$O_2 + 4(H^+ + e^-)$	-195.562	4.920	0.000

Table S6 The calculation details of the Gibbs free energy change of the intermediate product in monolayer SnP during the OER. Here, E_{DFT} represents the total energy of the intermediate product adsorbed at the most probable position on the superlattice surface, G_{tot} represents the total Gibbs free energy, and the T is set to 298.15 K.

Materials	E_{DFT}	ΔE_{zpe}	$T\Delta S$	Molecular	G_{tot}	$\Delta G(U = 0.0\ V)$	$\Delta G(U = 1.23\ V)$
G*	-159.228	0.000	0.000	H_2O	-187.696	0.000	0.000
G*OH	-169.092	0.321	0.097	$H_2O + (H^+ + e^-)$	-186.505	1.273	0.043
G*O	-165.802	0.074	0.068	$H_2O + 2(H^+ + e^-)$	-186.837	0.859	-1.601
G*OOH	-173.198	0.367	0.162	$3(H^+ + e^-)$	-183.203	4.734	1.044
G*	-159.228	0.000	0.000	$O_2 + 4(H^+ + e^-)$	-182.776	4.920	0.000

Table S7. The band edge calculation results for the three monolayers calculated by EN method. The intermediate quantities involved include the absolute electronegativity (χ) of each atom and material, as well as the band gap (E_g) calculated based on HSE06 functional. E_{CB} and E_{VB} correspond to the conduction band minimum (CBM) and valence band maximum (VBM), respectively. The atomic electronegativity here is referenced from the website www.knowledgedoor.com.

Materials	Absolute electronegativity (eV)			E_g (eV)	E_{CB} (eV)	E_{VB} (eV)
	Si/Ge/Sn	P	χ			
SiP	4.77	5.62	5.18	2.50	-3.93	-6.43
GeP	4.60	5.62	5.08	1.98	-4.09	-6.07
SnP	4.30	5.62	4.92	1.85	-3.99	-5.84

References

[1] W. Fang, K. Kuang, X. Xiao, H. Wei, Y. Chen, M. Li, Y. He, J Alloy Compd, 2023, 931, 167586.
[2] W. Fang, X. Xiao, H. Wei, Y. Chen, M. Li, Y. He, Materials Today Communications, 2022, 30, 103183.
[3] X. Lv, W. Wei, Q. Sun, F. Li, B. Huang, Y. Dai, Applied Catalysis B: Environmental, 2017, 217, 275-284.
[4] X.-F. Sheng, X.-X. Rao, C. Ke, W.-B. Kang, Applied Surface Science, 2022, 601, 154166.
[5] P. Zhang, J. H. Yuan, W. Y. Fang, G. Li, J. F. Wang, Applied Surface Science, 2022, 601, 154176.
[6] D. H. Ozbey, M. E. Kilic, E. Durgun, Physical Review Applied, 2022, 17, 034043.
[7] Z. Haman, N. Khossossi, M. KibbouI, l. Bouziani, D. Singh, I. Essaoudi, A. Ainane, R. Ahuja, Applied Surface Science, 2021, 556, 149561.